AD-A134 250   AN INVESTIGATION OF THE TEXTURE SURFACE SILICON SOLAR   1/ ᵭ
               CELL(U) FOREIGN TECHNOLOGY DIV WRIGHT-PATTERSON AFB OH
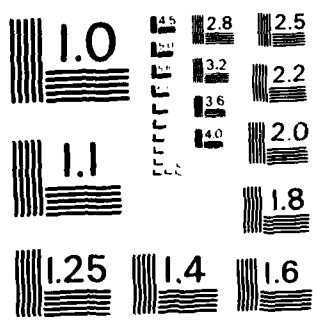   C RONGQIANG ET AL. 06 OCT 83 FTD-ID(RS)T-1392-83
UNCLASSIFIED   F/G 10/2   NL

END
DATE
FILMED

DTIC

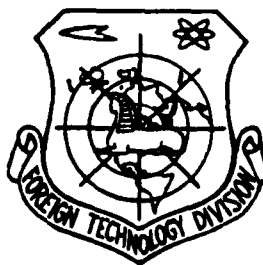| | 1.0 | | 2.8 | 2.5 |
			3.2	2.2
			3.6	
			4.0	2.0
	1.1			
				1.8
	1.25	1.4		1.6

MICROCOPY RESOLUTION TEST CHART
NATIONAL BUREAU OF STANDARDS-1963-A

FOREIGN TECHNOLOGY DIVISION

AN INVESTIGATION OF THE TEXTURE SURFACE SILICON SOLAR CELL

by

Cui Rongqiang and Qin Huilan

EDITED TRANSLATION

AN INVESTIGATION OF THE TEXTURE SURFACE SILICON
SOLAR CELL

By: Cui Rongqiang and Qin Huilan

GRAPHICS DISCLAIMER

All figures, graphics, tables, equations, etc.
merged into this translation were extracted
from the best quality copy available.

i

AN INVESTIGATION OF THE TEXTURE SURFACE SILICON SOLAR CELL

Cui Rongqiang and Qin Huilan
(Xian Jiaotong University)

Abstract

This paper analyzes and discusses the optical and electri-
cal properties of the texture surface silicon solar cell. A
new method of etching a texture surface by LiOH is presented
and the mechanism of etching a texture surface is investigated.

I. Preface

Use of the preferential etching properties of etching
solution causes the surface of the [100] silicon to form a
rough surface from a series of pyramid orientation permutations.
The reflection loss is greatly reduced because of the many
reflections and refractions of the light within the pyramid
(see table 1) and the utilization ratio of light is increased.
This type of rough surface looks like velvet and is therefore
called a "texture surface." The cell made with a texture sur-
face is called a "texture surface cell" [1] as well as a "non-
reflective cell" or "black cell." In recent years, foreign
nations have combined "texture surface" technology with "violet
cells", "back electric fields" and other technology. They have
raised the AMO efficiency of silicon solar cells to 18% and the
terrestrial efficiency was raised to 22% [2] so that the texture
surface cell was second to none among high efficiency cells. A
square matrix made up of large disk texture surface cells has
already been put into terrestrial use. Research on texture
surface cells is significant for raising the efficiency of
existing solar cells and lowering costs.

1

(1)电池类型	(4)无抗反射膜	(6)单层抗反射膜	(8)多层抗反射膜	(9抗反射膜加有机封装
(2)光面	(5)约 35%	(7)约 10%	7%	—
(3)绒面	10%	3—4%	—	4—5%

Table 1 Comparison of the mean reflectivities of the texture
surface and optical surface cells.

Key: (1) Type of cell; (2) Optical surface;
(3) Texture surface; (4) Without antireflective
film; (5) About; (6) Single layer antireflective
film; (7) About; (8) Multilayered antireflective
film; (9) Antireflective film with organic seal.

The special structure of the surface of the texture surface
cell has a tremendous effect on the optical and electrical
properties of the entire cell as well as the firmness of the
electrode. This paper will analyze and discuss these charact-
eristics. It will also introduce the method of etching a
texture surface by LiOH and carry out a preliminary investiga-
tion of the mechanism of etching a texture surface.

II. The Surface Structure and Optical Properties of a Texture
Surface

Fig. 1(a) is an ideal longitudinal section of a texture
surface cell and Fig. 1(b) is a longitudinal section of an
optical surface cell. Looking at Fig. 1(a), we know from cal-
culating the crystalline structure of the monocrystal silicon
that the vertex angle of each pyramid is $70°32'$.

When light with one beam intensity of I_o is separately pro-
jected vertically on a texture surface and an optical surface,
reflection and refraction will occur on the silicon surface.
On the texture surface, I_o produces reflected light I_1 and
refracted light I_2 at point A; I_1 continuously produces quad-
ratic reflected light I_1' and refracted light I_2' at point B

(Fig. 1(a)). They separately satisfy the following relation-
ships [3].

[Page(s) missing from original].

There is a complex functional relation which exists between
this collection efficiency and the diffusion length (or life) of
the charge carrier and absorption coefficient of the light.
However, we can qualitatively analyze the reason for the en-
largement of the section cell's short circuit current.

(1) Because the pyramid surface of the tetragonal pyramid
is $\sqrt{3}$ times larger than the bottom surface, the texture sur-
face cell has a p-n junction area $\sqrt{3}$ times larger than that
of the optical surface cell. This will increase the collection
of photon-generated carriers and thus increase the short cir-
cuit current.

(2) Based on the fundamental principle of the photovoltaic
effect, the actual output of the photon-generated current forms
a direct ratio with the photon-generated carrier number which
is separated by the electric field established in the p-n
junction near the p-n junction. Because of the refraction of
light on the texture surface, the greater portion of photons
are absorbed relatively close to the p-n junction. Therefore,
photon-generated carriers are also produced relatively close to
the p-n junction and are easily separated by the p-n junction.
Secondly, it is also advantageous to collect photon-generated
carriers along the pyramid valley formed from the p-n junction
of the pyramid surface which reduces recombination and in-
creases the short circuit current.

(3) Because of surface refraction, the optical path in the
texture surface piece is 1.5-2 times longer than the optical
path in the optical surface piece. This raised the probability
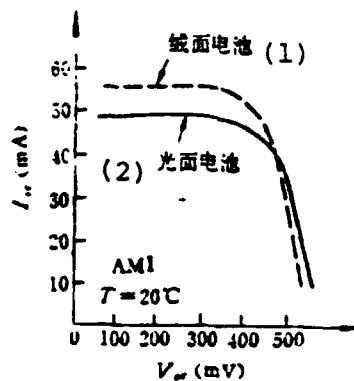of producing photon-generated carriers and thus raised the

3

short circuit current.

Fig. 5   Photoelectric properties of a 1×2cm^2 texture surface
         cell and an optical surface cell.

         Key: (1) Texture surface cell; (2) Optical surface
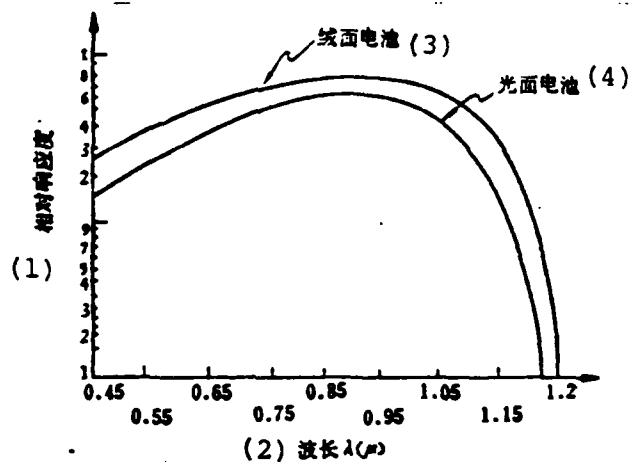   cell.

Fig. 6   Relative spectral responses of the texture surface
         cell and optical surface cell.

         Key: (1) Relative responsivity; (2) Wavelength;
         (3) Texture surface cell; (4) Optical surface cell.

2.   Open-Circuit Voltage

Broana and Brandhorst used a scanning electron microscope
to obtain a texture surface cell's diode response pattern
[4] (Fig. 7).   It can be seen from Fig. 7(a) that the

4

relative responsivity in the area of the pyramid valley is higher than in the area of the peak. Broana et al explained this phenomenon as follows: "An oversaturated doped dead layer possibly exists in the peak area and the valley area is possibly a low doped area which has a response higher than that of the peak area." This is one possible reason yet other reasons also possibly exist. We can see from Fig. 3 that the light density distribution on the pyramid surface is heterogenous and the light intensity of the valley area is larger than the light intensity of the peak area. This will cause the valley area's photoelectric current intensity to be larger than the photoelectric current intensity of the peak area. The open-circuit voltage is

$$V_{oc} = \frac{AkT}{q} \ln\left(\frac{I_e}{I_o} + 1\right)$$

We know from the above formula that under the same I_o conditions, the V_{oc} of the valley area is higher than the V_{oc} of the peak area.

Furthermore, we can see from Fig. 7(b) that the probability of photon-generated carriers collecting at point B of the valley area is greater than at the point A of the peak area. If we use minority carrier diffusion length 1 as the radius and separately use A and B as the centrally drawn arc to obtain two fan-shaped areas, we can separately express the probability of the A and B areas collecting minority carriers of diffusion length 1. Naturally, the ratio of the two fan-shaped areas is equivalent to the ratio of the two included angles and the specific value is approximately equal to 4 (i.e. $\frac{360^\circ - 70^\circ 32'}{70^\circ 32'} = 4$). This is also to say that the probability of the valley bottom p-n junction collecting photon-generated carriers is four times that of the peak area. This should also be the reason why the valley area has a higher response than the peak area.
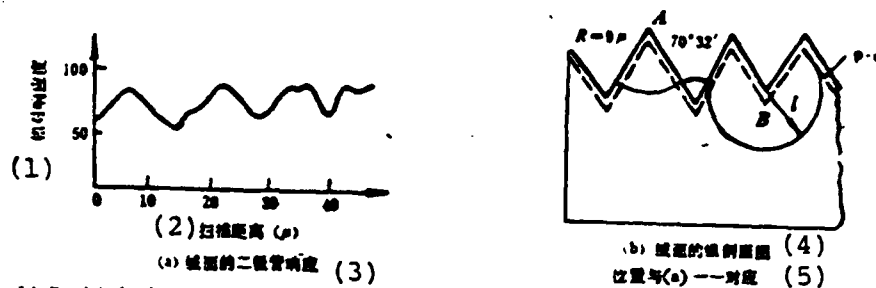
5

(1)

(2) 扫描距离 (µ)

(3)

(4)

(5)

Fig. 7   Response pattern of the texture surface cell's diode
         obtained by a scanning electron microscope.

Key: (1) Relative responsivity; (2) Scanning distance;
(3) Diode response of texture surface; (4) Longitud-
inal section of texture surface; (5) Position with
(a)--corresponding.

3.   Spectral Response

The so-called spectral response is the ratio of the photo-
electric current collected by each wavelength and the number of
photons falling on the surface.

In the silicon chip, the light follows the absorption
theorem,

$$I=I_o e^{-ax}$$

In the formula, I is the light intensity of area x (see
Fig. 1), I_o is the light intensity of the x=0 area and a is
the absorption coefficient.

Lights with different wavelengths have different a values
(Fig. 8). Because the forbidden band transition of silicon is
indirect, therefore a changes relatively slowly with the wave-
length. Among these, the violet light area a is maximum and
the red-infrared light area a is relatively small. The violet
light area is basically completely absorbed in the $x=1\mu$ m
area; for the red-infrared light area, only in the area wherein
x equals one to several hundred micron can it be fully absorbed.

6

Because of the reduction of the texture surface cell's reflection loss, the total quantity of violet light to infrared light entering the silicon chip is increased. Therefore, the spectral response of the violet light to infrared light is improved. Moreover, because the optical length in the texture surface cell is long, therefore the increase of the red light response is even more noticeable.
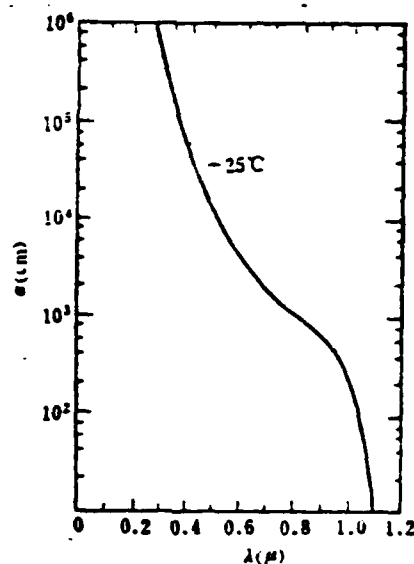

Fig. 8   The absorption coefficient a follows the wavelength distribution.

IV.   The Electrode of the Texture Surface Cell

We know from the analysis of the preceding section that the surface area of the texture surface cell is $\sqrt{3}$ larger than that of the optical surface cell (see Fig. 1). Thus, any one grid wire (including the main grid and fine grid) with the same width on the electrode will have a contact area $\sqrt{3}$ times larger on the texture surface than on the optical surface. It can generally be considered that the firmness of the grid wires is in direct ratio with the contact area of the grid wires and silicon and therefore the electrode firmness of the texture surface cell is $\sqrt{3}$ times higher than that of the optical surface cell. Following the electrode on the pyramid being able to sustain the pulling force of each direction, the

7

firmness of the electrode was further raised. This allowed the texture surface cell to be able to use electrode manufacturing techniques with costs lower than those for vacuum vapor plating such as electroplating, chemical plating, silk screen printing etc.

The contact resistance of the texture surface cell electrode is smaller than that of the optical surface. Because the contact resistance of the electrode is distributed resistance determined by the metal-semiconductor contact layer, in most situations, the contact resistance of the electrode is in direct ratio to the metal-silicon contact area. We can see from this that with the same width of metal grid wire, the contact resistance on the texture surface will be $\sqrt{3}$ times smaller than that of the optical surface.

V. Obtaining the Texture Surface and an Investigation of the LiOH Etching Mechanism

The silicon monocrystal is a type of crystal with a diamond structure [5]. Figure 9 shows a space cubic lattice made up of the eight silicon atoms of A B C D E F G H. The six atoms a b c d e f are its face-center and this is a face-centered cubic cell. We take R as an apex angle of another face-centered cubic cell (not drawn in) which with the above mentioned cell has a space of 1/4 BH on the diagonal line BH. Moreover, we take the R atoms as central which with the four atoms of Babe form a covalent bond. If ABFG is the [100] crystal face, then the crystal face determined by abe is [111]. In the same way, the crystal faces determined by bce, cde and dae are also [111]. By using certain etching solutions for the preferential etching of different crystal faces, we can etch out the tetragonal pyramids of four [111] faces on the [100] face. This tetragonal pyramid is the basic structure of the texture surface.
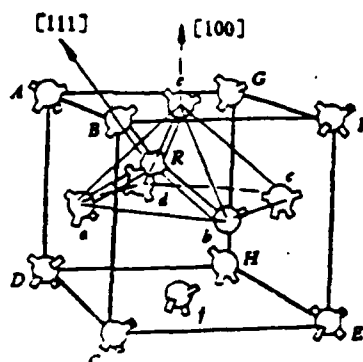
8

Fig. 9   Diamond structure of **the silicon** monocrystal.

Braona and Brandhorst used KOH and diamine (etching solutions 3* and 4* in Table 2) to etch silicon and successfully obtained a texture surface [4]. We used 1* and 2* etching solutions on a [100] silicon monocrystal plate and likewise obtained a texture surface (see Table 2). We also researched the etching solutions with different compositions and different compound ratios. The etching conditions and surface conditions of the silicon chip influenced etching results.

The etching results were that the surface often had very heterogenous etching spots and in order to solve the problems of insufficient blackness etc. we must analyze the etching mechanism.

The chemical reaction in an LiOH aqueous solution is

(1)

$$Si + 2LiOH + H_2O \xrightarrow{\text{加热}} Li_2SiO_3 + 2H_2\uparrow$$

Key: (1) Heating

9
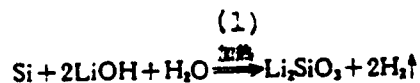
(1)序 号	成 份(2)配 比	(3)腐 蚀 条 件
1	LiOH(0.7%—1%)＋乙醇(10%—15%) (4)	电炉加热，80℃投片，添加乙醇，93℃—97℃腐蚀6—20分 (8)
2	NaOH(1%)+乙醇(15%)(5)	电炉加热，85℃投片，添加乙醇，90℃—95℃腐蚀6—30分 (9)
3	联胺(50%) (6)	电炉煮沸时间大于6分 (10)
4	KOH(1.4%)+去离子水 (7)	电炉加热，80℃—85℃腐蚀10分 (11)

Table 2 Preferential etching solution and etching conditions.

Key: (1) Number; (2) Composition and compound ratio; (3) Etching conditions; (4) Ethyl alcohol; (5) Ethyl alcohol; (6) Diamine; (7) Deionized water; (8) Electric furnace heating, 80° projected slice, added ethyl alcohol, 93°C-97°C etching for 6-20 minutes; (9) Electric furnace heating, 85°C projected slice, added ethyl alcohol, 90°C-95°C etching for 6-30 minutes; (10) Electric furnace boiling time greater than 6 minutes; (11) Electric furnace heating, 80°C-85°C etching for 10 minutes.

As for the monocrystal silicon, the atomic density of the [111] crystal face is maximum, distribution is uniform and the surface can be minimum (i.e. the most stable) and therefore relatively difficult to etch. The [100] surface, however, is the opposite and is easy to etch. In this way, the same type of etching solution has very different speeds for different crystal faces. This is so-called preferential etching. If the silicon reacts in an LiOH etching solution with a concentration greater than 5%, the greater part of the OH⁻ions cover the preferential etching properties and the obtained etching is a bright silicon surface. Therefore, the texture surface can only be obtained in an LiOH aqueous solution. Tests discovered that the preferential etching properties of diluted LiOH and NaOH solutions are similar.

Based on the theory of surface absorption, after the silicon chip enters the solution, the etched silicon surface completely

absorbs a layer of molecules and an ion layer and among them the Li^+, OH^- and H^+ each have certain concentrations. Because of the differences of the silicon chips surface states as well as the randomness of the molecular movement, at certain points in this absorption layer the above chemical reactions can occur and the ions produced by the reactions changed the composition of the absorption layer. If we want the reaction to continue, we must move the SiO_3^{--} and H_2 and provide new OH^- etc. All of this must depend on the thermal motion of the molecules and ions for completion. Tests prove that only when $T > 70°C$ is the thermal motion sufficiently strong and then the etching can obtain the texture surface.
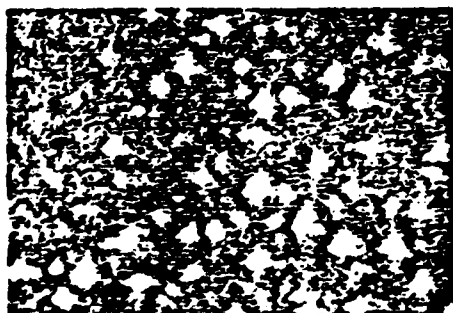
The addition of anhydrous alcohol in the etching solution can change the surface tension of the silicon and etching solution, lower the absorption of H_2 by the silicon surface, cause the H_2 to easily escape and thus overcome the "spots" and obtain a satisfactory texture surface.
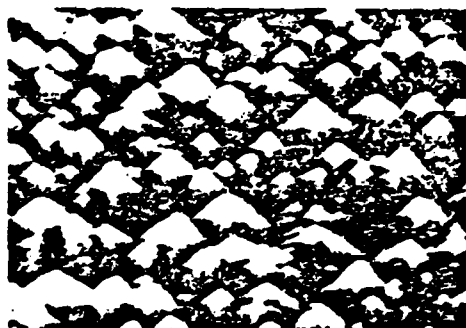
(a)95°C 12分 (1)
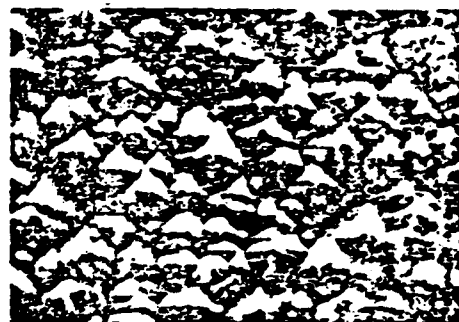
(b)95°C 15分 (2)

(c)95°C 19分 (3)

(d)95°C 19分 +97°C 5分 (4) (5)

Fig. 10 (see next page)

11

Fig. 10   LiOH etched texture surface (SEM 1250x)
          Key: (1) Minutes; (2) Minutes; (3) Minutes;
          (4) Minutes; (5) Minutes.

It can be seen from Fig. 10 that the texture surface pyramid
dimensions are mostly between 5-15 μm and the minimum is even
below 1 μm. The size intervals are random yet all abide by
Ayuyi's law of the conservation of crystal face angle and the
included angles between the corresponding two random adjoining
crystal faces are equal. At the same time, it was discovered
that when we use different etching solutions and different
etching conditions to obtain the texture surface, many pyramid
ruptures and incomplete phenomena exist. It can be deduced
from this that because of certain random factors, the etching
caused already existing pyramids to continuously corrode, break
and disintegrate and new pyramids to continuously form and
grow. If this be the case, after a certain time the average
dimensions of the pyramid are only related to temperature and
concentration but not to time. Moreover, during this process,
the breaking, disintegrating and forming of the pyramids are
continuous.

Tests initially prove the above inferences. Figure 10
consists of photographs of a silicon chip surface etched by
LiOH. The photographs were taken by a scanning electron micro-
scope. It can be seen from the photographs that after the
temperature is maintained at 95°C and the silicon chip is separ-
ately etched for 12, 15 and 19 minutes the sizes of the pyramids
are very close; for the silicon chip which has already been
etched for 19 minutes in a 95°C solution, after the temperature
of the solution rises to 97°C and there is continuous etching
for 5 minutes, the dimensions of the pyramids noticeably en-
large. If we let h indicate the mean height or mean valley
depth (the two are equal) of the pyramid, then within a certain
temperature range, h is the certain type of function of

12

solution temperature T:hocf(T). However, f(T) is related to the mean kinetic energy of the molecules and ions in the etching solution.

The breaking and incompleteness of the pyramids will increase the reflection loss and scattering loss of light, harm the homogeneity of the p-n junction and directly influence cell quality. Raising the completeness of the pyramid is the key to improving texture surface cell quality.

VI. Conclusion

1. The texture surface cell has small reflectivity, the collection efficiency of photon-generated current is high, its radiation-resistant properties are good, its capabilities for the absorption and scattering of light are strong, the electrode is firm etc. It also has potential for raising cell efficiency and lowering costs.

2. By using the LiOH etching solution we can obtain a satisfactory texture surface. When in an etching solution with fixed concentration, within a certain time the main dimensions of the pyramids on the texture surface will only be related to the temperature of the etching solution but almost unrelated to the time.

3. The p-n junction of the texture surface cell is $\sqrt{3}$ times as large as that of the optical surface. The effect of the condition of the p-n junction on the cell's properties is very great. When a shallow junction is made on the texture surface and there is a fine grid and Ta_2O_5 antireflective film, this can improve the cell's properties.

4. When we increase the lighting of the texture surface cell, this can possibly raise the open-circuit voltage and efficiency of the texture surface cell.

13

References

[1] R. A. Arndt et al., Optical properties of the nonreflective cell, Conf. Rec. of the 11th IEEE photovol special conf. Scottsdale, Arizona, May 6-8, 1975.

[2] Harold J. Hovel, Solar Cells for Terrestrial Applications, IBM Corporation.

[3] Fukuri Shi and Kibo Rewa, General Physics, translated by the Physics Department of Dongbei People's University, Higher Education Press, 1955.

[4] Braona and Brandhorst, V-Grooved Silicon Solar Cell, Conf. Rec. of the 11th IEEE photovol Special Conf. Scottsdale, Arizona, May 6-8, 1975.

[5] Xie Xide, Fang Junxin, Solid Physics, Shanghai Science and Technology Press, 1962.

DTIC